

## Response of granular superconducting $\text{YBa}_{2.1}\text{Cu}_{3.4}\text{O}_{7-x}$ to light

J. C. Culbertson, U. Strom, S. A. Wolf, and W. W. Fuller

*Naval Research Laboratory, Washington, D.C. 20375*

(Received 19 November 1990; revised manuscript received 26 July 1991)

We report measurements performed on a granular  $\text{YBa}_{2.1}\text{Cu}_{3.4}\text{O}_{7-x}$  film which are consistent with a transition to the zero-resistance state that can be described as a two-dimensional transition in terms of the Kosterlitz-Thouless formalism. A photoresponse associated with this transition is interpreted in terms of a photon-assisted vortex-antivortex unbinding process.

### I. INTRODUCTION

There has been recent interest<sup>1-10</sup> in understanding the photoresponse of high-temperature superconductors. The emphasis in most of these studies [2-10] is on high quality films for which the photoresponse is not dominated by intergrain boundary effects. The fundamental issue is whether films made of materials such as  $\text{YBa}_2\text{Cu}_3\text{O}_{7-x}$  exhibit the same nonequilibrium properties as have been demonstrated for low-temperature superconductors<sup>11</sup> such as Pb and, more recently,<sup>12</sup> Nb. Although there have been a great number of experimental investigations, the issue is still unresolved.

The present paper is concerned with films of high-temperature superconductors for which intergrain boundaries are expected to play a very large role. There is much experimental evidence that granular films have a distinctly different photoresponse compared to homogeneous superconducting films. Early work by Rose and co-workers<sup>13</sup> established that films of granular Sn exhibited a response to microwaves that was greatly enhanced over that exhibited by homogeneous films having lower resistances. Enomoto *et al.*<sup>14</sup> observed similar effects using visible and infrared light for  $\text{BaPb}_{0.7}\text{Bi}_{0.3}\text{O}_3$  films. Both experiments have been interpreted in terms of the response predicted for a disordered array of Josephson junctions. In particular, Enomoto *et al.* argued that the absorption of visible light in the superconducting grains results in an increase in the quasiparticle concentration which acts to depress the superconducting gap, which in turn would alter the critical current of the boundary Josephson junctions that exist between the superconducting grains.

The specific two-dimensional character of films has been invoked to explain transport measurements on thin superconducting films<sup>15-18</sup> and, more recently, to explain photoresponse measurements of very thin granular  $\text{NbN}/\text{BN}$  films.<sup>19</sup> The behavior of the current-voltage curves and the photoresponse of such films were interpreted in terms of a process involving the binding and unbinding of magnetic flux vortices and antivortices.<sup>1,19</sup> Such a process is likely mediated by phonons if the photons incident on the film have energies that are substantially greater than the superconducting energy gap of the film. For photons having energies below the gap, the

direct coupling of the photon's fields to the superconducting current in the junctions between the grains is possible.<sup>19</sup> These qualitative proposals for the photon-vortex interaction have been extended by Kadin *et al.*<sup>20-22</sup> to include not only vortex-antivortex pair dissociation, but also the possibility that the absorption of a single photon can give rise to the creation of a vortex-antivortex pair that can in turn be swept out by the fields of the current and thus give rise to a signal. This model is analogous to semiconductor detectors where an absorbed photon creates an electron-hole pair, which is swept out by the applied fields. Kadin, Leung, and Smith<sup>20</sup> also suggested that light could be absorbed in a small superconducting contact between grains, causing transient local heating which acts to depress the critical current and allows one or more phase slips to occur.

In the present paper we report a detailed investigation of the photoresponse of a granular film of  $\text{YBa}_{2.1}\text{Cu}_{3.4}\text{O}_{7-x}$  whose transition to zero resistance is well described by Kosterlitz-Thouless- (KT-) type vortex dynamics. The paper extends on previously published preliminary data<sup>1</sup> by presenting new time-resolved photoresponse measurements in the 10–100-ns range and the 1- $\mu\text{s}$  to 0.1-s range. The results confirm our earlier interpretation<sup>1</sup> of the faster photoresponse component observed near the KT transition in terms of a vortex unbinding process.

### II. EXPERIMENTAL DETAILS

Unless otherwise mentioned, the following data refer to measurements performed on a 2500-Å-thick film of granular  $\text{YBa}_{2.1}\text{Cu}_{3.4}\text{O}_{7-x}$ , which was deposited (using radio-frequency magnetron sputtering) onto a MgO substrate. This film was annealed in an oxygen atmosphere at 900 °C for 10 min and then annealed for 5 h at 450 °C. The final composition given above was measured using elastic backscattering. A scanning electron microscope showed that the film was composed of randomly oriented grains on the order of 0.7  $\mu\text{m}$  in size in a porous network. A four-point probe pattern was created with a current path width of 2 mm. Electrical contact was made with evaporated silver pads, which were attached with small indium dots to the copper wires.

The film was weakly transparent (about 10% transmis-

sion, 80% absorption at 6328 Å) to visible light. Two different light sources were used: (1) a steady-state 1-mW He-Ne laser, which was chopped from 1 Hz to 20 kHz, and (2) a pulsed (10-ns pulse width) nitrogen-pumped dye laser. The laser-beam profiles were of comparable diameter to the length and width of the current path in the film.

The photoresponse measurements were carried out under conditions where the sample was cooled with He gas in a Dewar with optical access. The sample was in good thermal contact with a copper holder whose temperature was measured with a Si diode. Further experimental details have been described previously.<sup>1</sup>

### III. EXPERIMENTAL RESULTS

#### A. Transport measurements

Figure 1 shows the resistance of the  $\text{YBa}_{2.1}\text{Cu}_{3.4}\text{O}_{7-x}$  film as a function of temperature for a bias current of 0.25 mA ( $\sim 50 \text{ A cm}^{-2}$ ). The superconducting transition temperature on the grains in the film is  $T_{cg} \sim 82 \text{ K}$ . The resistance above  $T_{cg}$  decreases as the temperature is raised; this thermally activated behavior is a characteristic of the conduction of granular films.<sup>15,16</sup> The temperature at which the film resistance drops precipitously toward zero is  $T_c \sim 12 \text{ K}$ . As the temperature decreases from  $T_{cg}$  to  $T_c$ , the phases of the superconducting order parameters of the individual grains gradually order; when the temperature reaches  $T_c$ , enough of the grains are phase ordered to form a continuous superconducting pathway between the electrical contacts on the sample.

Figure 2 shows the results of current-voltage measurements performed in the dark for a range of temperatures from 8 K (below  $T_c$ ) to 20 K (above  $T_c$ ). The current region from 1 to 2 mA was fit to a power law  $V = aI^n$ ; the power-law exponents from these fits listed in the figure range from  $n = 1.6$  to 4.3. The current-voltage curves at lower currents deviated from power-law behavior due to

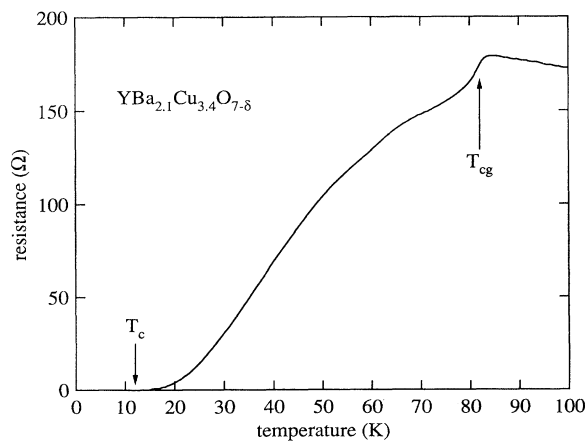


FIG. 1. Film resistance measured as a function of temperature for a bias current of 0.25 mA. Note the labeled temperatures:  $T_{cg}$  at which the grains in the film go superconducting and  $T_c$  at which the resistance of the film as a whole reaches zero.

thermal voltages that were not subtracted out; the measurement was made for only one polarity of current; the size of the offset that would transform the current-voltage curve for  $T = T_c$  to a pure power law is on the same order as the subsequently measured thermal voltages.

#### B. Photoresponse

Figure 3 shows the photoresponse measured as a function of temperature for four bias currents: 0.25, 0.5, 1, and 2 mA. These measurements were made using the steady-state light source chopped at a frequency of 3 kHz. With each of these measurements of photoresponse and all others in this paper, we made simultaneous measurements of the resistance of the film. Generally, the dc voltage across the sample was much larger than the photoresponse signal. The film resistance was also measured as a function of temperature for several bias currents with the sample in the dark. The derivative of the measured resistance with respect to temperature,  $dR/dT$ , is shown for the case of a 2-mA bias current. The peak at 82 K and the peak just above 60 K are associated with the superconducting-to-normal transitions of the two phases of superconductor that are present in this sample. The photoresponse above 20 K varies linearly with bias current and has features which are mirrored in the measured  $dR/dT$ . This is an indication that this portion of the photoresponse is bolometric in nature. For a

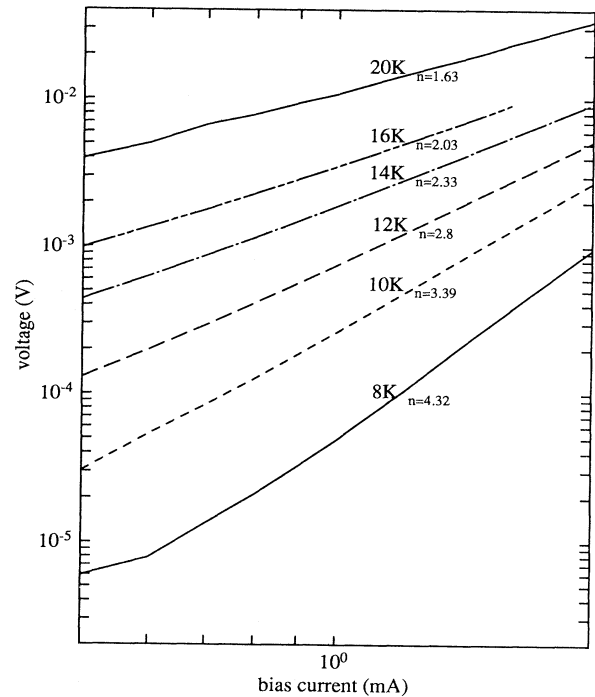


FIG. 2. Voltage across film measured as a function of bias current for six different temperatures from 8 to 20 K. The voltage-current region between 1 and 2 mA was fit to a power law; the exponents resulting from these fits are listed next to the temperatures at which the curves were measured. A cubic power law is obtained for a temperature of 11.23 K.

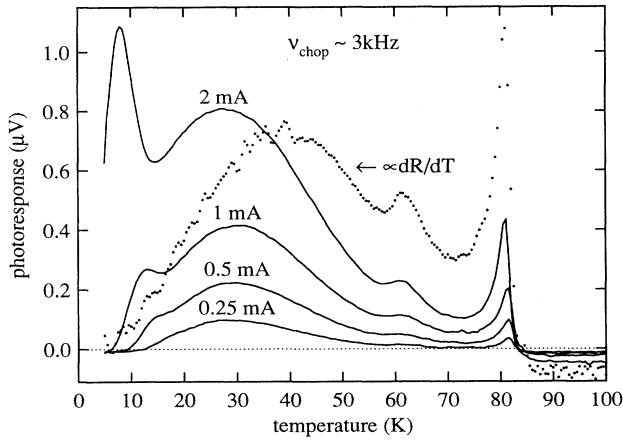


FIG. 3. Photoresponse measured as a function of temperature in response to a 1-mW steady-state He-Ne laser chopped at 3 kHz. The photoresponse measured for four different bias currents are shown (0.25, 0.5, 1, and 2 mA). Also shown is a curve proportional to the temperature derivative of the measured film resistance that was measured with the bias current equal to 2 mA.

bolometric photoresponse the voltage change  $\delta V_{\text{bol}}$  is related to the temperature rise  $\delta T$  by

$$\delta V_{\text{bol}} = \delta(IR) = I \left[ \frac{\partial R}{\partial T} \right] \delta T, \quad (1)$$

where  $\delta T$  is the temperature rise in the film caused by the absorption of light. Whenever photons are absorbed by a detector, its temperature will rise, and if the property being measured changes with temperature, there will be a bolometric photoresponse; this is true whether or not other mechanisms (nonbolometric) exist that yield a photoresponse. The responsivity for a resistance bolometric detector is defined as the ratio of the photoresponse voltage to the input light power. For the case where thermal conduction away from the region where the light is absorbed is dominated by a single thermal time constant  $\tau$ , the responsivity is<sup>23</sup>

$$r_{\text{bol}} = F \left[ \frac{\partial R}{\partial T} \right] I / [\kappa_e (1 + \omega^2 \tau^2)^{1/2}], \quad (2)$$

where  $F$  is the fraction of the incident light that is actually absorbed,  $\omega$  is the angular frequency of the measurement, the thermal time constant  $\tau = C/\kappa_e$ ,  $C$  is the appropriate effective specific heat of the bolometer, the effective thermal conductance is  $\kappa_e = \kappa - I^2(\partial R/\partial T)_I$ , and  $\kappa$  is the pertinent or limiting thermal conductance of the bolometer;  $C$  and  $\kappa$  are in units of J/K, and W/K, respectively. In the limiting case  $\omega\tau \ll 1$ , the responsivity  $r_{\text{bol}} \propto 1/\kappa_e$  is independent of frequency. In the opposite limit,  $\omega\tau \gg 1$ , the responsivity  $r_{\text{bol}} \propto 1/(\omega C)$  decreases with increasing frequency. For measurements made on longer and longer time scales, the bottleneck in heat transport may occur further and further away from the point at which the light was absorbed, in regions composed of different materials. Thus it is possible to have

different thermal time constants dominate bolometric photoresponse measurements made on different time scales.

Specific heats and thermal conductivities generally vary with temperature. Thus thermal time constants may shift with temperature. We observe that thermal time constants at lower temperatures correspond to faster cooling. This is demonstrated in Fig. 4, which shows a photoresponse measurement made using the steady-state light source chopped at 15 kHz and a bias current of 0.75 mA. Figure 4 also indicates the measured resistance and its derivative.

Figure 5 shows measurements of the photoresponse as a function of chopping frequency that were made for five different temperatures: 28, 20, 15, 10, and 8 K. The light source was a 1-mW He-Ne laser. In the frequency range below 10 kHz, the thermal time constants are seen to move to higher frequencies as the temperature is lowered. From 1 to 10 kHz, where the photoresponse is independent of frequency, the heat conduction out of the sample is limited by the thermal conductivity of the MgO substrate. The  $\omega^{-1}$  region between 100 and 1000 Hz is associated with the heat transfer from the MgO substrate to the Cu cold finger of the Dewar. To determine the average increase in temperature for a given laser power, the chop frequency must be lowered until the measured  $\delta V$  no longer increases; this  $\delta V$  along with Eq. (1) implies a given temperature rise for a laser power  $P$ . When the chopping frequency is high compared to the thermal relaxation rate, then the average laser power is  $P/2$  (assuming equal chopper-block-chopper-unblock times), and so the time-averaged increase in temperature can be obtained by measuring the photoresponse at slow chopping

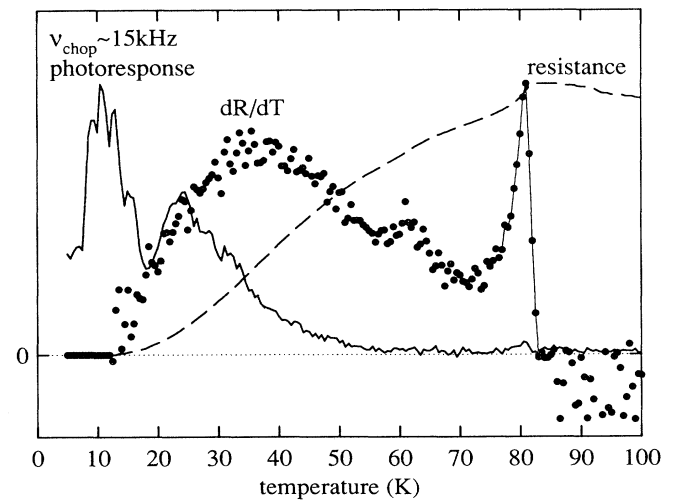


FIG. 4. Photoresponse measured as a function temperature in response to a 1-mW He-Ne laser chopped at 15 kHz. Also shown is the resistance  $R$  measured as a function of temperature and its temperature derivative  $dR/dT$ . Note the reduction of the bolometric response features that are proportional to  $dR/dT$  at all but the lowest temperatures where the thermal time constants for the bolometric photoresponse are still comparable or faster than the chopping period.

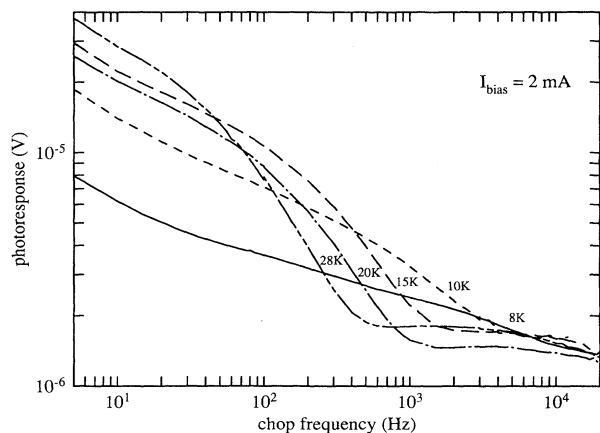


FIG. 5. Photoresponse measured as a function of the frequency  $\nu$  at which the 1-mW He-Ne laser was mechanically chopped. The measurements were performed for five temperatures between 8 and 28 K. A bias current of 2 mA was used for all of the measurements. Note that the  $1/\nu$  fall offs and the constant response plateaus characteristic of bolometric response for the higher-temperature measurements. The lowest-temperature photoresponse measurements do not fall off as  $1/\nu$ , which suggests the existence of an additional photoresponse which may not be bolometric in nature.

rates and at half laser power. For example, at 20 K, using a bias current of 2 mA and a light chopping frequency of 3 kHz, we find, using Eq. (1), that  $\delta T = 0.16$  mK, whereas the time-averaged increase in the film temperature is approximately 6 mK.

The  $\omega^{-1}$  region just above 10 kHz is associated with the heat transfer from the  $\text{YBa}_{2.1}\text{Cu}_{3.4}\text{O}_{7-x}$  film to the MgO substrate. Note that the 10- and 8-K curves never change as fast as  $\omega^{-1}$ . This implies that at these temperatures there is a faster photoresponse component added to the bolometric components mentioned above. This faster component is *frequency independent* (at least up to 20 kHz). After subtracting the fast component from the 10- and 8-K data, we obtain an approximate  $\omega^{-1}$  response falloff. This frequency-independent photoresponse exists only at the lower temperatures (below 20 K) and corresponds to the peak in the photoresponse which is observed at low temperatures near the resistive onset  $T_c$ . It is this feature in the photoresponse that will be focused on henceforth and whose nonequilibrium nature is considered in the next section.

The response to a 10-ns long pulse of 5839 Å wavelength light ( $\sim 1 \mu\text{J}$  absorbed per pulse in a spot having a 3-mm diameter) is shown in Fig. 6 as a function of temperature. There are no obvious photoresponse features left that correspond to features in  $dR/dT$ . Only the peak near  $T_c$  remains.

#### IV. DISCUSSION

##### A. Kosterlitz-Thouless transition

Studies of the Kosterlitz-Thouless phase transition in granular films have predicted the functional form of the

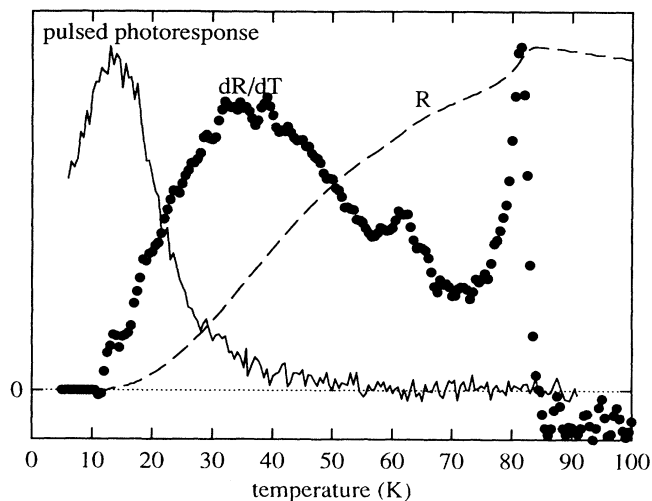


FIG. 6. Photoresponse measured as a function of temperature in response to pulsed light of 10 ns duration ( $\sim 1 \mu\text{J}$  absorbed per pulse of 5839-Å-wavelength light in a spot having a 3-mm diameter). Also shown is the measured resistance  $R$  and its temperature derivative  $dR/dT$ . At this measurement speed there are no obvious features in the photoresponse that are proportional to  $dR/dT$ .

voltage-current relation<sup>1,15-17</sup> for temperatures around the transition temperature to be  $V \propto I^n$ , where  $n = 3.0$  at  $T = T_c$  for small currents and  $n = 1$  at  $T > T_c$ . The data shown in Fig. 2 are consistent with the predicted  $I$ - $V$  curves. It should be emphasized that the gradual, as opposed to abrupt, change in the exponent  $n$  with temperature is due to the granular nature of the film.<sup>15,16</sup> We determine  $T_c = 11.23$  K, corresponding to the temperature for which  $V \propto I^{3.0}$ .

The predicted form of the resistance for low currents just above the Kosterlitz-Thouless transition is<sup>15</sup>

$$R/R_{\max} = a \exp[-2(b/\tau)^{1/2}], \quad (3)$$

where  $\tau \equiv (T - T_c)/(T_{cg} - T)$  and  $R_{\max}$  is the film resistance at the temperature just above  $T_{cg}$  where it reaches a maximum. The theory<sup>15</sup> also relates both  $a$  and  $b$  to the dielectric constant  $\epsilon$  for the vortex-antivortex system; this relation depends on the intergranular charging (capacitive) effects. Figure 7 shows a plot of a measurement of the film resistance just above  $T_c$  made using a bias current of 20  $\mu\text{A}$ . These data, fit to Eq. (3) using  $T_{cg} = 82$  K and  $T_c = 11.23$  K, resulted in  $a = 3.77$  and  $b = 0.82$ . The fit is displayed as a line in the figure. In the theory of the Kosterlitz-Thouless transition, adapted to the case of granular superconducting films, the fitting parameters  $a$  and  $b$  are not dependent.<sup>15</sup> Viewed with a scanning electron microscope, these high- $T_c$  samples are seen to be made of large grain sizes ( $\sim 0.7 \mu\text{m}$ ). These large grain sizes suggest that intergranular charging effects are not important in the calculation of dielectric constant. The values of  $a$  and  $b$  implied by such a calculation are consistent with the values of  $a$  and  $b$  quoted above for a dielectric constant  $\epsilon = 2.07$ . It should be noted that the calculation makes use of a less extreme approxima-

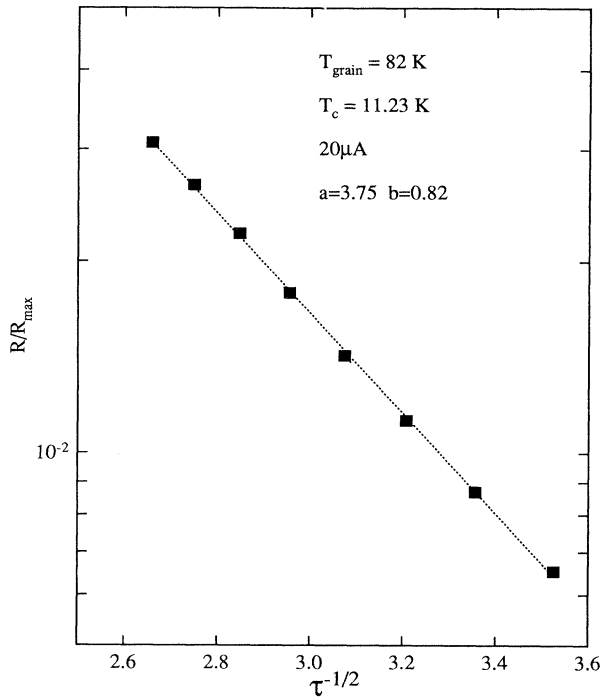


FIG. 7. Plot of the fit of the resistance just above the Kosterlitz-Thouless transition temperature to a functional form that is predicted using by theory ( $R/R_{\max} = a \exp[-2(b/\tau)^{1/2}]$ , where  $\tau \equiv (T - T_c)/(T_{cg} - T)$  and  $R_{\max}$  is the film resistance at the temperature just above  $T_{cg}$  where it reaches a maximum).

tion<sup>15,16</sup> for the Josephson coupling energy than that commonly used when dealing with superconducting materials that have  $T_c \sim T_{cg}$ . Ying and Kwok<sup>24</sup> have recently interpreted their voltage-current measurements for a  $\text{YBa}_2\text{Cu}_3\text{O}_{7-\delta}$  film in terms of a Kosterlitz-Thouless transition. For their high quality polycrystalline film ( $T_c = 83.45$  K,  $T_{cg} = 85.95$  K), they deduce a value of  $\epsilon = 2.4$ . A somewhat larger value of  $\epsilon$  was estimated by Fiory *et al.*<sup>25</sup> using a different experimental technique for films that were more homogeneous than the film investigated here.

In summary, the above data are consistent with the existence of a Kosterlitz-Thouless transition occurring in the neighborhood of 11 K. The values of the parameters  $a$  and  $b$  obtained from the data imply a vortex dielectric constant  $\epsilon \approx 2.1$ , which is consistent with other experiments. The relative magnitudes of  $a$  and  $b$  imply that intergranular charging effects do not play a significant role, consistent with the grain sizes in the film observed by scanning electron microscopy.

### B. Nonequilibrium photoresponse

We propose to separate the photoresponse as follows:

$$\delta V = \delta V_{\text{bol}} + \delta V_x, \quad (4)$$

where  $\delta V_{\text{bol}}$  is bolometric in nature and the nature of  $\delta V_x$ , the photoresponse peak near  $T_c$ , is to be addressed.

The group of phenomena that are accepted by the su-

perconductivity community as being of a nonequilibrium superconductive nature includes the following: an energy distribution of quasiparticles that is not in thermal equilibrium (characterized by a quasiparticle self-thermalization time constant), a quasiparticle energy distribution that is not in thermal equilibrium with the Cooper pairs (characterized by a quasiparticle to Cooper-pair recombination time), an energy distribution of phonons that is not in thermal equilibrium (included because phonons intermediate the standard superconducting interaction), and branch or charge imbalance in the quasiparticle distribution (the distribution of quasiparticles having energies above the gap is not in thermal equilibrium with the distribution of quasiparticles having energies below the superconducting gap). One should add nontraditional excitations to this list, such as nonthermal distributions of magnetic-flux vortices and antivortices. We suspect that the photoresponse peak that we observe near  $T_c$  is caused by light perturbing the distribution of magnetic-flux vortices away from equilibrium.

The two contributions  $\delta V_{\text{bol}}$  and  $\delta V_x$  can be separated on the basis of different temperature dependences, response times, and dependences on bias current. It is clear from Fig. 3 that the photoresponse near the KT transition increases faster than linearly with bias current, in contrast to the photoresponse measured at higher temperature, which increases linearly with bias current. The component of the photoresponse that depends superlinearly on current is shown in Fig. 8. The superlinear part was isolated by using the photoresponse measured at the lowest bias current to subtract off the low-current-limit component of the photoresponse from the three highest bias-current measurements. If the photoresponse were bolometric, then Eq. (1) and the voltage-current relation ( $V \propto I^n(T)$ ) appropriate for the currents used imply that the photoresponse near the Kosterlitz-Thouless transition depends nonlinearly on the bias current as  $\delta V \propto I^{n(T)} \ln(I) [\partial n(T)/\partial T] \delta T$ ; at  $T_c$  a bolometric photoresponse should increase with current faster than cubically. Instead, we observe that the photoresponse at  $T_c$  depends quadratically on the current; the photoresponse is proportional to the differential resistance  $\partial V/\partial I$ . The observed dependence of the amplitude of the photoresponse on current is not consistent with that expected for a bolometric photoresponse.

Further evidence for a nonequilibrium response comes from the temperature dependence of the photoresponse. In Fig. 9(a) the 15-kHz photoresponse data shown in Fig. 4 is replotted on a logarithmic scale. It is clear from Fig. 9(a) that the peak in the photoresponse corresponds very closely to the temperature ( $\sim 12$  K) where the resistance of the film drops abruptly. If one assumes that the photoresponse is bolometric, then Eq. (1) and the signals measured in Fig. 9(a) are sufficient to determine the magnitude of the 15-kHz modulation in temperature  $\delta T$  caused by the absorption of the incident chopped light. The result is plotted in Fig. 9(b). Above 25 K we find that  $\delta T \propto T^{-3}$  is reasonably accurate. This temperature dependence is consistent with the predictions of Eq. (2) using the information of the frequency dependence of the

photoresponse in Fig. 5. The dominant thermal factor in this frequency range for temperatures greater than 25 K is the specific heat of the MgO substrate. Thus, according to Eq. (2),  $r_{\text{bol}} \approx F(\partial R / \partial T)I / (\omega C_{\text{MgO}})$ , and using Eq. (1),  $\delta T \propto 1/(\omega C_{\text{MgO}})$ . In this temperature range  $C_{\text{MgO}} \propto T^3$  and  $\delta T \propto T^{-3}$  in agreement with Fig. 9(b). The magnitude of the temperature rise calculated using the specific heat of MgO and the geometry of the sample agrees with that shown in Fig. 9(b) for  $T > 25$  K. As seen in Fig. 9(b), the equilibrium thermal behavior implied for  $T > 25$  K is in distinct contrast to that implied for  $T < T_c$ . If the photoresponse for  $T < T_c$  is interpreted in terms of a bolometric mechanism, then there must be a light-induced temperature rise which increases by more than three orders of magnitude as  $T$  is lowered from just above to just below  $T_c$  (the quantity  $\delta V / |\partial V / \partial T|$  without the absolute values oscillates positive and negative because the derivative is zero within the noise and so the  $\delta T$  inferred is a lower bound). The  $\geq 1$ -K temperature rise implied by the assumption that the photoresponse is bolometric for  $T < T_c$  is unreasonably high. The temperature rise obtained by extrapolating the solid curve in Fig. 9(b) to 10 K is less than 1 mK. Thus the large enhancement of the low- $T$  photoresponse cannot be explained by an increase in the effective bias temperature of the film. These data are then inconsistent with the assumption that the low-temperature ( $< 10$ -K) photoresponse is bolometric in nature.

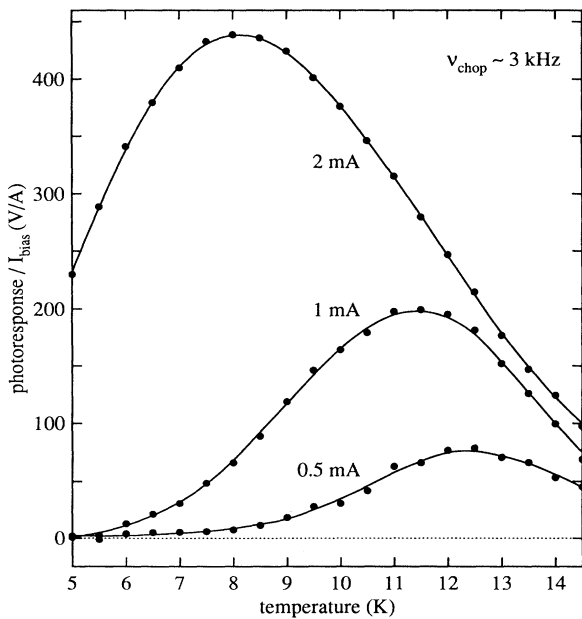


FIG. 8. Replot of the photoresponses measured in Fig. 3 as a function of temperature, but with the components that vary linearly with bias current subtracted out. The photoresponses are plotted normalized by the bias currents of the respective measurements (0.5, 1, and 2 mA; the 0.25-mA curve was used to produce these curves).

The pulsed photoresponse data shown in Figs. 10–12 provide us with additional evidence for a nonequilibrium mechanism. In Fig. 10 the pulsed photoresponse data are shown as a function of temperature for three different bias currents. The data appear similar to  $\delta V_x$  measured at 3 kHz (Fig. 3); however, upon closer examination the photoresponse peaks measured for pulsed light are broader and shifted to higher temperatures; furthermore, the photoresponse becomes proportional to the square of the bias current not at 11 K, but at 5 K. These effects can be understood in terms of the larger temperature rise induced by the higher-intensity pulsed light, which will be discussed in detail below.

The time dependence of the pulsed photoresponse in Fig. 11 reveals some very interesting facts in regard to the nature of the nonequilibrium mechanism. All photoresponse amplitudes have been scaled so as to compare shapes. The solid, dashed, and dotted curves are, respectively, the photoresponse measurements made in first 40 ns after the start of the 10-ns laser pulse, in the next 30 ns, and from 2.5 to 5  $\mu$ s after the laser pulse. The solid circles refer to the 15-kHz data (Fig. 4), the open circles to the 3-kHz data from which the slower bolometric com-

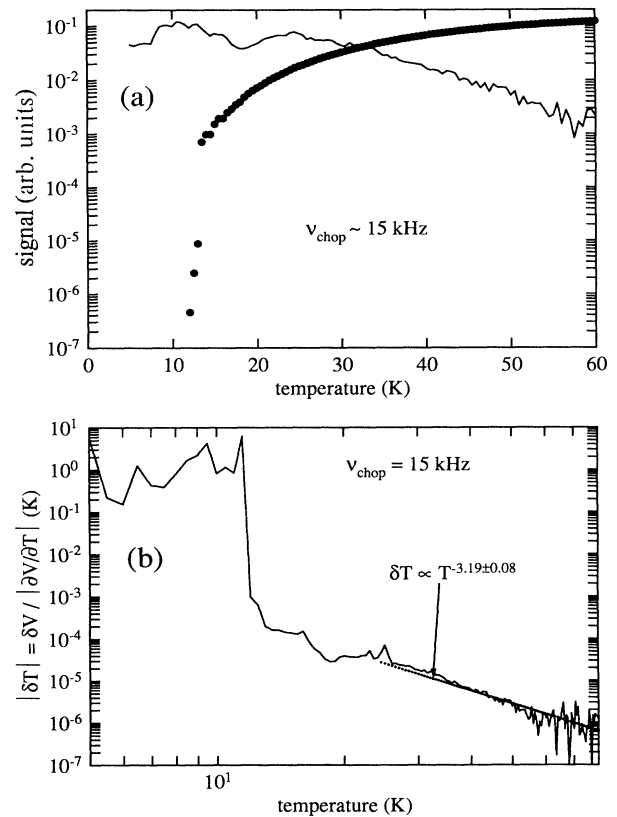


FIG. 9. (a) Photoresponse (solid line) and resistance (dots) data of Fig. 4 replotted semilogarithmically to illustrate that the photoresponse near 10 K is being measured where the film resistance approaches zero. (b) Data  $[\delta V(T)]$  of (a) expressed as a temperature rise  $\delta T = \delta V / |\delta V / \delta T|$ .

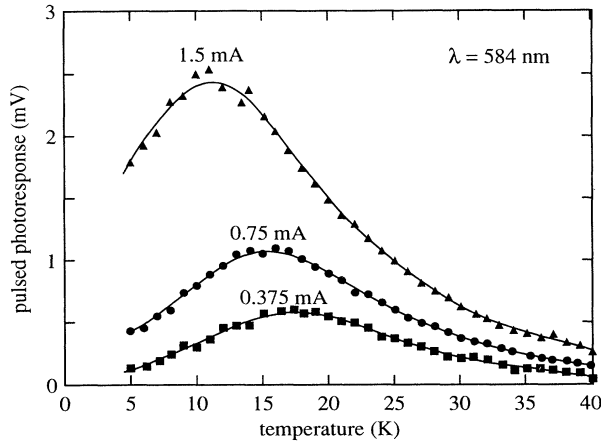


FIG. 10. Photoresponse measured as a function of temperature in response to pulsed light. The three curves were measured for bias currents of 1.5 mA (triangles), 0.75 mA (circles), and 0.375 mA (squares).

ponent has been subtracted (Fig. 8). The most significant result is that the temperature dependence of the pulsed photoresponse measured between 40 and 70 ns after the start of the 10-ns laser pulse is identical, within experimental error, with the photoresponse measured using a 1-mW He-Ne laser chopped in the 15-kHz range. The temperature dependence of the pulsed photoresponse relaxes completely to that of the 15-kHz photoresponse in less than 30 ns after the end of the 10-ns laser pulse. The photoresponse measured from 1 to 5  $\mu\text{s}$  after the laser pulse shows a less pronounced peak near  $T_c$ . Over the temperature range from 10 to 20 K, we observe three different photoresponses that behave distinctly

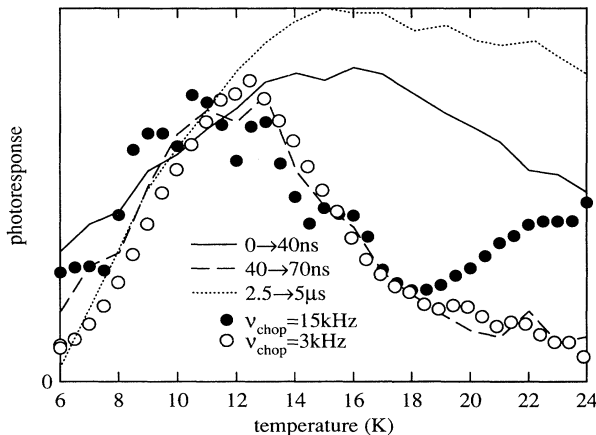


FIG. 11. Photoresponse as a function of temperature measured for a range of time scales: 1-mW steady-state source chopped at 3 kHz (open circles) and 15 kHz (solid circles); a 10-ns pulsed light source with the photoresponse measured in the first 40 ns (solid line) after the laser pulse started, during the next 30 ns (dashed line), and from 2.5 to 5  $\mu\text{s}$  after the laser pulse (dotted line). The amplitudes of the various measurements have been adjusted to illustrate shapes.

differently: the slow bolometric photoresponse, the intermediate speed photoresponse which peaks near  $T_c$ , and the fastest photoresponse which occurs on time scales comparable to the duration of the light-induced temperature rise caused by absorption of short pulses of light.

The size and duration of the temperature rise caused by the absorption of a 10-ns pulse of light can be estimated by using an “equilibrium” thermal model. At temperatures near 10-K, photons absorbed within one optical absorption depth from the incident surface are on the order of one phonon mean free path from the film-substrate boundary.<sup>26</sup> Given typical phonon velocities in  $\text{YBa}_{2.1}\text{Cu}_{3.4}\text{O}_{7-x}$  it takes times on the order of tens of picoseconds for a phonon to cross the film. The phonon scattering in the substrate is much weaker,<sup>27</sup> and the mean time between phonon scattering events is on the order of 100 ns; until several 100 ns, no significant number of phonons will have been scattered back from the MgO to the film-MgO boundary, and so diffusion in MgO on these short-time scales is not pertinent. The process limiting heat transport out of the film at low temperatures and fast-time scales is the transport of heat across the film-MgO boundary; this can be described in terms of a blackbody radiation problem,<sup>28</sup> at an ambient temperature of 11 K, we estimate that the temperature of the superconducting film will increase by 4.5 K; the decay back to the ambient temperature is characterized by the thermal relaxation time  $\tau = C(T)/K(T)$ , where  $C(T)$  is the heat capacitance of the film and  $K(T)$  is the heat conductance per unit area of the film/substrate interface. The heat capacity<sup>26</sup> per unit area for a  $\text{YBa}_2\text{Cu}_3\text{O}_{7-x}$  film of thickness  $d$  is  $C(T) = C_v(T)d = 8.5 \times 10^{-8} T^3 \text{ J cm}^{-2} \text{ K}$  and the thermal conductance<sup>28</sup>  $K(T) \approx 0.05 T^3 \text{ W cm}^{-2} \text{ K}$ . Hence  $\tau = C(T)/K(T) = 1.7 \times 10^{-9} \text{ s}$ . By fitting an exponential to our pulsed photoresponse decay curves, we estimate an experimental value for  $\tau \approx 35 \text{ ns}$  (for the decay curve around 40 ns after the laser pulse). The estimated film-cooling time of 1.7 ns assumes an equilibrium phonon distribution and neglects phonon scattering at the superconducting-film-dielectric interface due to roughness, contamination, and scattering of phonons from the bulk of the MgO back to the interface. For most dielectrics such factors contribute to enhancement of the cooling decay time by a factor of 3. This suggests that the fast relaxation of the temperature dependence of the pulsed photoresponse may follow the heating of the film, but that the photoresponse peak at  $T_c$  that depends superlinearly on current has other origins (i.e., is nonbolometric).

The above discussion assumes that the phonons resulting from the absorption of photons rapidly decay to a blackbody distribution of phonons. If such an assumption is not valid and the energy distribution of phonons remains skewed toward higher energy phonons (that have very slow group velocities), then a thermal transport bottleneck in the thermalization could be realized. Thermal bottlenecks are well known for crystalline<sup>29,30</sup> and amorphous<sup>31,32</sup> semiconductors. This phenomena could give rise to a slower heat loss from the film than that estimated above.

Finally, in Fig. 12, the pulsed photoresponse is

displayed as a function of bias current. The photoresponse was measured for the first 40 ns after the start of the laser pulse (solid curves) and for the following 30 ns (dashed curves). These measurements were repeated for three temperatures around the temperature  $T_c$ , where the film resistance vanishes for low bias currents: (a) 5 K, which is below  $T_c$ ; (b) 11 K, which is approximately equal to  $T_c$ ; and (c) 20 K, which is above  $T_c$ . Above  $T_c$  the shape of the photoresponse versus temperature measurement does not change with time. At  $T_c$  the delayed measurement of the photoresponse (dashed curve) when fit to a power law in bias current (photoresponse  $\propto I^n$ ) yields a power-law exponent  $n = 1.98 \pm 0.04$ ; at  $T_c$  the differential resistance of the film is quadratic in bias current; the photoresponse measured during the laser pulse can be modeled as the sum of two terms: one depending linearly and one depending quadratically on bias current. The linear component decays away completely within 30 ns after the laser pulse. Below  $T_c$  the delayed measurement of the photoresponse has a threshold

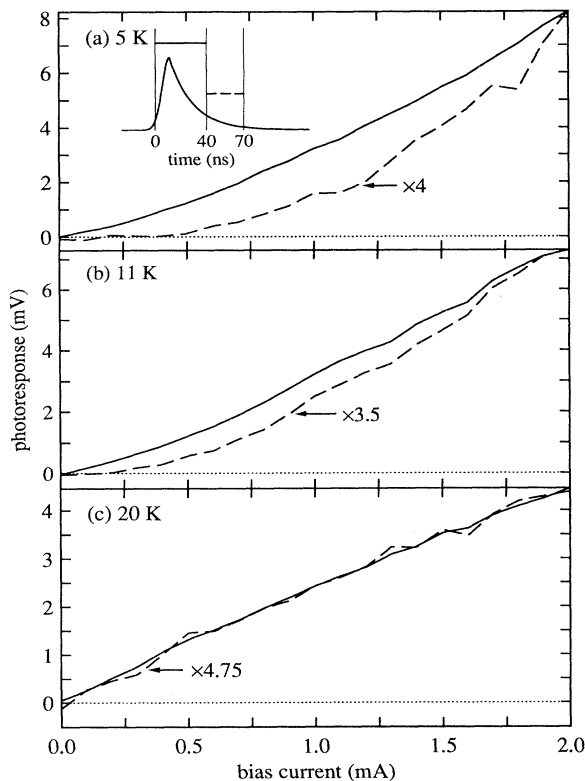


FIG. 12. Photoresponse measured as a function of bias current in response to a 10-ns pulse of visible light. The measurement was repeated for three different temperatures: (a) 5 K, which is below  $T_c$ ; (b) 11 K, which is approximately equal to  $T_c$ ; and (c) 20 K, which is above  $T_c$ . The photoresponse was measured both in the first 40 ns (solid lines) and in the subsequent 30 ns (dashed lines); the start of the 10-ns laser pulse corresponds to zero time. Note the change in relative behavior of the two photoresponse measurements as the temperature changes from below  $T_c$  to above  $T_c$ .

current and increases faster than quadratically with  $I - I_{\text{threshold}}$ . The current dependences of the delayed photoresponse in these temperature regimes are consistent with this being a nonequilibrium response associated with a Kosterlitz-Thouless transition.

### C. Microscopic models

The principal conclusion of the previous section was that a nonequilibrium photoresponse has been observed in a granular film of  $\text{YBa}_{2.1}\text{Cu}_{3.4}\text{O}_{7-x}$  near the temperature  $T_c$  where the transition to the zero-resistance state is thought to be dominated by vortex dynamics. It has been previously proposed<sup>1,19,33</sup> that such a nonequilibrium photoresponse is likely due to the dissociation of bound vortex-antivortex pairs. Evidence for such a process has been presented<sup>1,19</sup> for thin granular films of NbN/BN and  $\text{YBa}_{2.1}\text{Cu}_{3.4}\text{O}_{7-x}$ . The nature of the coupling of the light to the vortices is subject to speculation.

Kadin and co-workers<sup>20-22</sup> recently pointed out that in addition to the dissociation of existing vortex-antivortex pairs, the incoming light may actually create vortex-antivortex pairs. The mechanism by which light couples to these excitations is envisioned in terms of a localized “hot” region which is created by the absorption of incident photons. Kadin *et al.*<sup>21</sup> have proposed that the current responsivity for this process is given by

$$R = \phi_0/hf = 1/2ef, \quad (5)$$

where  $\phi_0$  is the unit flux quantum and  $hf$  is a quantum of light, and a quantum efficiency of unity is assumed. We also expect that Eq. (5) represents an upper bound for the unpairing of existing, bound vortices. For light with  $hf = 1$  eV, the theoretical responsivity is  $\sim 1.3 \times 10^4$  V/W. In addition to the predicted responsivity, the vortex-flow mechanism is expected to be relatively fast. Typical vortex speeds<sup>21</sup> are on the order of  $10^7$  cm/s. For dimensions of  $10 \mu\text{m}$  the predicted speed limited by vortex motion over that distance is  $10^{-10}$  s. For our 0.2-cm-wide current path, the vortex transit time could be as fast as 20 ns.

High responsivities ( $\sim 6000$  V/W for 0.6- $\mu\text{m}$  photons) have been reported<sup>21,34</sup> for thin NbN films which were patterned into micrometer-wide meander paths. The present  $\text{YBa}_{2.1}\text{Cu}_{3.4}\text{O}_{7-x}$  film displayed a much smaller responsivity of about 0.1 V/W at 10 K. One possible explanation is that few of the photons incident on our film are “effective” in unbinding a vortex-antivortex pair. The present film has large micrometer-sized grains, which implies relatively fewer weak links per unit area than the NbN/BN films with 100- $\text{\AA}$  grain sizes. In addition,  $\text{YBa}_{2.1}\text{Cu}_{3.4}\text{O}_{7-x}$  has a sizable absorption due to charge transfer processes in the 2-eV spectral region (NbN is relatively transparent in this spectral range). This absorption can occur in crystalline regions without significant effect on the resistive properties of the film. With regard to response speed, the rise time of the pulsed photoresponse was within our 10-ns resolution. The fall time of the pulse was several tens of nanoseconds for  $T < T_c$ . These response times are not inconsistent with the vortex-unbinding mechanism if one takes into ac-



count the large dimensions of the film, making it unlikely that a free vortex will cross the sample without recombining or becoming bound and thereby reducing the expected responsivity as well as the response speed.

## V. CONCLUSION

We have seen evidence for the occurrence of a Kosterlitz-Thouless transition in a granular Y-Ba-Cu-O superconducting film that has a wide normal ( $T_{cg} \approx 82$  K) to zero-resistance ( $T_c \approx 11$  K) transition: The current-voltage relation behaves as predicted as a function of temperature. Fitting the temperature dependence of the film resistance just above  $T_c$  to the theoretically expected form yields self-consistent fitting parameters.

A photoresponse is seen that is associated with a Kosterlitz-Thouless transition. It is seen only in the temperature region near  $T_c$ . Measurements performed as a function of bias current demonstrate that the amplitude of the photoresponse is proportional to the differential resistance  $dV/dI$ ; this current dependence is inconsistent with the photoresponse being bolometric. This conclusion is supported by measurements made on different times scales (from steady-state light to mechanically chopped light with increasing frequency to pulses of light of 10-ns duration). Instead, a nonequilibrium mechanism

has been proposed which is dominant for  $T < T_c$ .

We speculate that the observed nonequilibrium photoresponse may be related to a mechanism by which local heating is induced in the contacts between grains. This local heating may unbind nearby pinned vortices, which in turn leads to resistive loss. A process by which local heating creates vortex-antivortex pairs is also possible.<sup>20</sup> Below  $T_c$  such a process will require a minimum bias current, which is consistent with experimental observation, but by no means demonstrates the nature of the photon-vortex interaction.

We believe that realistic modeling of the photoresponse can be realized with disordered arrays of Josephson junctions. Considerable progress has been made recently in modeling vortex-antivortex pair creation near defects in model junction arrays.<sup>35</sup> The perturbing influence of optical radiation on such model systems could, in principle, provide a microscopic model of the photon-vortex pair interaction.

## ACKNOWLEDGMENTS

We acknowledge helpful discussions with Mike Leung and, for film growth, P. Skeath. This research was supported in part by the Office of Naval Research and the Strategic Defense Initiative Organization.

- 
- <sup>1</sup>J. C. Culbertson, U. Strom, S. A. Wolf, P. Skeath, E. J. West, and W. K. Burns, *Phys. Rev. B* **39**, 12 359 (1989).
- <sup>2</sup>A. Frenkel, M. A. Saifi, T. Venkatesan, Chinion Lin, X. C. Wu, and A. Inam, *Appl. Phys. Lett.* **54**, 1594 (1989).
- <sup>3</sup>M. G. Forrester, M. Gottlieb, J. R. Gavaler, and A. I. Braginski, *Appl. Phys. Lett.* **53**, 1332 (1988).
- <sup>4</sup>W. S. Brocklesby, Don Monroe, A. F. J. Levi, M. Hong, S. H. Liou, J. Kwo, C. E. Rice, P. M. Mankiewich, and R. E. Howard, *Appl. Phys. Lett.* **54**, 1175 (1989).
- <sup>5</sup>E. Zeldov, N. M. Amer, G. Koren, and A. Gupta, *Phys. Rev. B* **39**, 9712 (1989).
- <sup>6</sup>H. S. Kwok, J. P. Zheng, Q. Y. Ying, and R. Rao, *Appl. Phys. Lett.* **54**, 2473 (1989).
- <sup>7</sup>R. Kaplan, W. E. Carlos, E. J. Cukauskas, and J. Ryu, *J. Appl. Phys.* **67**, 4212 (1990).
- <sup>8</sup>W. R. Donaldson, A. M. Kadin, P. H. Ballentine, and R. Sobolewski, *Appl. Phys. Lett.* **54**, 2470 (1989).
- <sup>9</sup>N. Bluzer, K. K. Fork, T. Geballe, M. R. Beasley, M. Reyzer, M. Johnson, S. R. Greenfield, J. Stankus, and M. Fayer, *IEEE Trans. Magn.* **MAG-27**, 1519 (1991).
- <sup>10</sup>S. G. Han, Z. V. Vardeny, O. G. Symko, and G. Koren, *IEEE Trans. Magn.* **MAG-27**, 1548 (1991).
- <sup>11</sup>L. R. Testardi, *Phys. Rev. B* **4**, 2189 (1971).
- <sup>12</sup>Mark Johnson, N. Bluzer, M. Reyzer, T. H. Geballe, S. R. Greenfield, John J. Stankus, M. D. Fayer, and C. Herring, *IEEE Trans. Magn.* **MAG-27**, 1523 (1991).
- <sup>13</sup>K. Rose, C. L. Bertin, and R. M. Katz, in *Applied Superconductivity*, edited by V. Newhouse (Academic, New York, 1975), Vol. 1, Chap. 4; C. L. Bertin and K. Rose, *J. Appl. Phys.* **42**, 631 (1971); R. M. Katz and K. Rose, *Proc. IEEE* **61**, 55 (1973).
- <sup>14</sup>Youichi Enomoto, Toshiaki Murakami, and Minoru Suzuki, *Physica C* **153-155**, 1592 (1988); Youichi Enomoto, Minoru Suzuki, and Toshiaki Murakami, *Jpn. J. Appl. Phys.* **23**, L333 (1984).
- <sup>15</sup>D. U. Gubser, S. A. Wolf, W. W. Fuller, D. Van Vechten, and R. W. Simon, *Physica B* **135** 131 (1985).
- <sup>16</sup>R. W. Simon, B. S. Dalrymple, D. Van Vechten, W. W. Fuller, and S. A. Wolf, *Phys. Rev. B* **36**, 1962 (1987).
- <sup>17</sup>B. I. Halperin and D. R. Nelson, *J. Low Temp. Phys.* **36**, 599 (1979).
- <sup>18</sup>K. Epstein, A. M. Goldman, and A. M. Kadin, *Phys. Rev. Lett.* **47**, 534 (1981).
- <sup>19</sup>U. Strom, J. C. Culbertson, S. A. Wolf, S. Perkowitz, and G. L. Carr, *Phys. Rev. B* **42**, 4059 (1990).
- <sup>20</sup>A. M. Kadin, M. Leung, and A. D. Smith, *Phys. Rev. Lett.* **65**, 3193 (1990).
- <sup>21</sup>A. M. Kadin, M. Leung, A. D. Smith, and J. M. Murduck, *Appl. Phys. Lett.* **57**, 2847 (1990).
- <sup>22</sup>A. M. Kadin, *J. Appl. Phys.* **68**, 5741 (1990).
- <sup>23</sup>P. W. Kruse, *Semicond. Sci. Technol.* **5**, S229 (1990).
- <sup>24</sup>Q. Y. Ying and H. S. Kwok, *Phys. Rev. B* **42**, 2242 (1990).
- <sup>25</sup>A. T. Fiory, A. F. Hebard, P. M. Mankiewich, and R. E. Howard, *Phys. Rev. Lett.* **61**, 1419 (1988).
- <sup>26</sup>Calculated using specific-heat and thermal-conductivity measurements in M. E. Reeves, D. S. Citrin, B. G. Pazol, T. A. Friedmann, and D. M. Ginzberg, *Phys. Rev. B* **36**, 6915 (1987); C. Uher, A. B. Kaiser, *ibid.* **36**, 5680 (1987).
- <sup>27</sup>Calculated using specific-heat and thermal-conductivity measurements in *Thermophysical Properties of Matter*, edited by Y. S. Touloukian, R. W. Powell, C. Y. Ho, and P. G. Klemens (IFI/Plenum, New York, 1970), Vol. 2, p. 166; and *Thermophysical Properties of Matter*, edited by Y. S. Touloukian and E. H. Buyco (IFI/Plenum, New York, 1970),

- Vol. 5, pp. 140–144.
- <sup>28</sup>R. E. Jones and W. B. Pennebaker, *Cryogenics* **12**, 215 (1963).
- <sup>29</sup>M. Greenstein, M. A. Tamor, and J. P. Wolfe, *Phys. Rev. B* **26**, 5605 (1982).
- <sup>30</sup>J. A. Shields and J. P. Wolfe, *Z. Phys. B* **75**, 11 (1989).
- <sup>31</sup>U. Strom, J. C. Culbertson, P. B. Klein, and S. A. Wolf, in *Phonon Scattering in Condensed Matter*, Vol. 51 of *Springer Series in Solid State Sciences*, edited by W. Eisenmenger, K. Lassmann, and S. Doettinger (Springer, New York, 1982), p. 339.
- <sup>32</sup>U. Strom, J. C. Culbertson, P. B. Klein, and S. A. Wolf, in *Optical Effects in Amorphous Semiconductors (Snowbird, Utah)*, Proceedings of the International Topical Conference on Optical Effects in Amorphous Semiconductors, edited by P. C. Taylor and S. G. Bishop, AIP Conf. Proc. No. 120 (AIP, New York, 1984), p. 157.
- <sup>33</sup>S. A. Wolf, U. Strom, and J. C. Culbertson, *Solid State Technol.* **33**(4), 187 (1990).
- <sup>34</sup>M. Leung (private communication).
- <sup>35</sup>W. Xia and P. Leath, *Phys. Rev. Lett.* **63**, 1428 (1989).